ELSEVIER

Journal of Structural Geology 29 (2007) 1241–1255

JOURNAL OF STRUCTURAL GEOLOGY

www.elsevier.com/locate/jsg

Multiple scales of mechanical stratification and décollement fold kinematics, Sierra Madre Oriental foreland, northeast Mexico

Diana K. Latta[1], David J. Anastasio*

Lehigh University, 31 Williams Drive, Bethlehem, PA 18015, USA

Received 10 June 2006; received in revised form 18 March 2007; accepted 19 March 2007
Available online 24 March 2007

Abstract

Regional- to outcrop-scale stratigraphic relationships within Mesozoic shallow marine carbonates and clastics at Sierra del Fraile anticlinorium in northeast Mexico play an important role in controlling the deformation distribution, strain history and kinematics during folding. Structural analyses of meso- and microscopic deformation features from all stratigraphic and structural positions within the anticlinorium allow for the delineation of five regional-scale lithotectonic units. Kilometer- to decameter-scale stacking patterns of the preorogenic succession and the meter-scale stacking patterns of individual shallowing-upward carbonate cycles are shown to influence deformation kinematics in predictable ways. Mesoscopic faults and cleavage patterns along with penetrative strain from anisotropy of magnetic susceptibility (AMS) fabrics constrain fold kinematics as progressive limb rotation about pinned anticlinal and synclinal hinges with constant limb length and a mobile basal décollement horizon within the evaporites of the Minas Viejas Formation that core the anticlinorium. AMS fabrics are shown to be a useful proxy for nascent penetrative strain orientations in sedimentary rocks. Macroscopic differences in strain suggest strong lithologic facies control responding to differences in bed thickness, grain size and carbonate content. At the regional scale, variation in deformation between the lithotectonic units identifies décollement horizons coincident with lithotectonic boundaries in the Minas Viejas, upper Taraises, and Parras Formations.

Keywords: Décollement fold; Lithotectonic units; Anisotropy of magnetic susceptibility; Mechanical stratigraphy; Mexico; Fold kinematics

1. Introduction

Many fold and thrust belts are composed of stratigraphic successions of mixed carbonate and clastic units deposited above thick evaporitic strata (e.g. Carpathians, Jura, Zagros, Pyrenees, Betics, Rif-Atlas, Salt Ranges, Sierra Madre Oriental). In such orogens, décollement (detachment) folding predominates over thrust faulting and both folds and faults display dual vergence (Dahlstrom, 1969, 1990; Jamison, 1987; Davis and Engelder, 1985). Previous empirical and theoretical studies of décollement folds have investigated the implications of constant (Epard and Groshong, 1993, 1995) versus variable (Dahlstrom, 1990; Epard and Groshong, 1995; Homza and Wallace, 1995, 1997) décollement depth, and fixed (De Sitter, 1956; Ramsay, 1967; Fisher and Anastasio, 1994; Hardy and Poblet, 1994; Epard and Groshong, 1995; Anastasio et al., 1997) versus migrating (Mitra and Namson, 1989; Dahlstrom, 1990) hinges on the resultant fold geometry, strain distribution, and deformation kinematics. These studies showed that geometry alone is insufficient to constrain fold kinematics. Inherent in a discussion of the deformation of sedimentary rocks is the relative roles that ductility or competency differences and the degree of anisotropy between folded layers have on deformation kinematics (Willis, 1892; Currie et al., 1962; Ramsay, 1967; Wood and Bergin, 1970; Johnson, 1980; Fischer and Jackson, 1999; Dixon, 2004).

Ductile and competent are terms often used by structural geologists to describe the relative strength of rock types. A

* Corresponding author. Fax: +1 610 758 3677.
E-mail addresses: diana.k.latta@exxonmobil.com (D.K. Latta), dja2@lehigh.edu (D.J. Anastasio).
[1] Present address: ExxonMobil Exploration Company, 233 Benmar Dr, Houston TX 77060, USA.

0191-8141/$ - see front matter © 2007 Elsevier Ltd. All rights reserved.
doi:10.1016/j.jsg.2007.03.012

ductile or incompetent rock penetratively deforms more readily than its neighbors, undergoes more finite strain before fracturing and flows in response to imposed geometric constraints (Elliott, 1981). Competent beds deform or flow less than incompetent beds, record less penetrative deformation, and fault before they fold (Dennis, 1967). For sedimentary rocks, the anisotropy provided by bedding is of paramount importance for the distribution of layer parallel shear during deformation. For both clastic and carbonate rocks, grain size and bedding thickness are related, with fine grain sizes in thin beds and coarse clastics typically organized in thick or massive beds (Pettijohn, 1975). Fine grained and thin-bedded rocks are more ductile than coarse grained and massively bedded rocks of the same composition (Ramsay, 1967). Lithologic heterogeneity is most easily organized in terms of sedimentary facies, which can be defined in terms of characteristic bed thicknesses, mineralogy and grain sizes.

The exposed Jurassic and Cretaceous units in Sierra del Fraile, Mexico vary in terms of their relative ductility. At a bed-scale, strain heterogeneity and multi-layer folding in the Mexican foreland suggests a typical lithologic competency series that decreases from dolomite, to limestone, sandstone, argillaceous limestone, shales, and evaporites. However, the stacking of the individual lithologic units into outcrop-scale and larger stratigraphy results in a lithotectonic stratigraphy that is not well explained by current paradigms. Changes in the competency of layers within a sequence can be manifested by heterogeneous strain distribution (e.g. Donath, 1962; Ramberg, 1963), wavelength of folds during folding (e.g. Nickelsen, 1963; Biot, 1964), boudinage geometry during extension (e.g. Ghosh, 1993), or the distribution and geometry of map-scale faults (e.g. Woodward and Rutherford, 1989). Whereas, differences in the anisotropy between layers, due to changes in bed thickness and foliation orientation also show a relative control on the portioning of strain (e.g. Donath, 1969; Williams, 1977). Stacking patterns of strata influence the distribution of strain over a range of spatial scales, from the kilometer-scale in an entire rift-drift succession, to the meter-scale in an individual shallowing-upward carbonate cycle, to the sub-meter scale of a single shale-carbonate couplet. Despite the early research works of Willis (1892) and Currie et al. (1962) there are relatively few studies that investigated the role lithotectonic units play in controlling strain distribution and folding. More recently, Fischer and Jackson (1999) and Higuera-Diaz et al. (2005) investigated the relationship between stratigraphy and deformation in a single fold complex in the Monterrey Salient, northeast Mexico.

In this paper, we characterize extensional fractures (joints and veins), shear fractures, stylolites and cleavage throughout the Sierra del Fraile anticlinorium (26°N 100°30′W) in the foreland of the Sierra Madre Oriental fold belt, in northeast Mexico. Sierra del Fraile is a large décollement fold, with a ~4.5 km thick clastic and carbonate section, deformed above a thick evaporitic sequence. Uncertainty exists in the thickness of the Mesozoic evaporite basin with estimates varying for ~1–2 km in the Monterrey Salient (Goldhammer et al., 1991) to <5 km thick in the La Popa Basin in the orogenic foreland (Wilson, 1990; Gray et al., 2001). Evaporites thicknesses surely varied across the basin much like today where salt welds and diapirism in La Popa basin bear evidence of halotectonics (Giles and Lawton, 2002). In the core of Potrero Garcia >3 km of evaporites were penetrated by an exploration well that did not reach the base of the section (Wall et al., 1961).

Mechanical stratigraphic units (*sensu* Donath and Parker, 1964), equivalent to lithotectonic units (*sensu* Currie et al., 1962) and structural lithic units (*sensu* Willis, 1892) refer to packages of sedimentary rock that display characteristic deformation features resulting from lithologic differences. Recognition of mechanical stratigraphy allows for better interpretations of fold geometry, cross section construction and restoration (Mountjoy, 1960; Dahlstrom, 1969; Wiltschko, 1979), and evaluation of reservoir quality (Mitra, 1987). The objectives of this paper are to: (1) describe the distribution and orientation of deformation features at the outcrop and grain size-scales throughout the anticlinorium in order to constrain fold kinematics, (2) use deformation distribution to define the lithotectonic units and differentiate scales of mechanical stratification, and (3) explore how lithologic variations and stratigraphic patterns affect strain history.

2. Geologic setting

In northeast Mexico, passive margin carbonates and clastics accumulated from the Late Jurassic through Middle Cretaceous in association with the opening of the Gulf of Mexico (Dickinson and Lawton, 2001). Clastic deposition continued into the Tertiary in response to the Sevier-Laramide orogeny (Longoria, 1998). Uplifted Paleozoic basement blocks and intervening grabens associated with continental rifting during the opening of the Gulf of Mexico (~210–165 Ma), played an important role in controlling depositional patterns along the Mexican Gulf Coast (Wilson, 1990; Dickinson and Lawton, 2001). At Sierra del Fraile, the Coahuila block influenced evaporite and carbonate facies distribution patterns and stratigraphy throughout the Early Cretaceous (Wilson, 1999).

Syn-rifting, thick sequences of Callovian age evaporites were deposited gulf wide; in northeast Mexico they comprise the Minas Viejas Formation (Pindell, 1985; Salvador, 1987). The mechanically weak evaporite deposits played an important role in controlling the geometries of Late Mesozoic-Early Cenozoic compressional structures associated with the Sevier-Laramide orogeny (Gray and Johnson, 1995; Marrett and Aranda-García, 1999). Folding in the foreland of the Sierra Madre Oriental fold belt, in the Coahuila Marginal Folded Province, is characterized by a series of NW-SE oriented, upright, roughly symmetric, doubly-plunging anticlines and synclines (Wall et al., 1961). The first order anticlines in the Coahuila Province are cored by the Minas Viejas Formation (Wall et al., 1961; Wilson et al., 1984). An exploratory well drilled in the hinge area of Potrero Garcia in Sierra del Fraile penetrated 610 m of gypsum and anhydrite, followed by 274 m of interbedded gypsum, anhydrite, and halite, all over 2134 m of pure halite without penetrating the entire section (Wall et al., 1961).

Jurassic age, medium- to thick-bedded limestones of the Zuloaga Formation lie unconformably above the Minas Viejas

evaporites, and conformably below the thin-bedded shales and limestones of the La Casita Formation in Sierra del Fraile (Fig. 1b,c). The Cretaceous age, thin-bedded shales and limestones of the Taraises Formation lie conformably above the La Casita Formation and grade conformably into thick-bedded limestones of the Cupido Formation, marking the onset of widespread carbonate platform development along the Gulf Coast margin (Wilson, 1999). By the earliest Cretaceous, extensive carbonate platforms developed around the entire Gulf of Mexico (Wilson, 1999). In northeastern Mexico, these platforms are represented by the Barremian-Aptian age Cupido Formation and the Albian age Aurora Formation each comprising a series of cyclic shallowing upward parasequences. The Aptian and Albian thick-bedded, reef sequences represent two distinct upward shoaling second-order megacycles separated by a second-order transgressive sequence within the cyclic carbonates of the upper Cupido Formation, and the thin-bedded, deeper-water shales of the La Peña Formation (Goldhammer et al., 1991) (Fig. 1b,c).

Conformably overlying the massive limestones of the Aurora Formation are the thin-bedded limestones and organic-rich shales of the Cuesta del Cura Formation, which lie conformably below the thin-bedded limestones and shales of the Indidura Formation (Fig. 1b,c). The deposition of the thin-bedded shales and thin interbedded sands of the Parras Formation mark the decline of the Cretaceous carbonate platforms around the Gulf of Mexico. The Parras Formation outcrops along the flanks of the Sierra del Fraile anticlinorium and in the surrounding synclinal valleys and is assumed to have covered the entire foreland of the Sierra Madre Oriental fold belt (McBride et al., 1974).

At Sierra del Fraile a majority of the ~4.5 km Mesozoic preorogenic succession is exposed providing an ideal setting to investigate the influence of stratigraphic packaging on strain accommodation during contractional deformation (Fig. 1). Deformation of the units exposed at Sierra del Fraile occurred at depths between 4.0 and 7.0 km, based on the maximum thickness of the Upper Cretaceous and Tertiary units interpreted above the anticlinorium, and temperatures less than 150 °C, based on fluid inclusion data from the Lower Cretaceous Cupido Formation in Potrero Garcia (Gray et al., 2001).

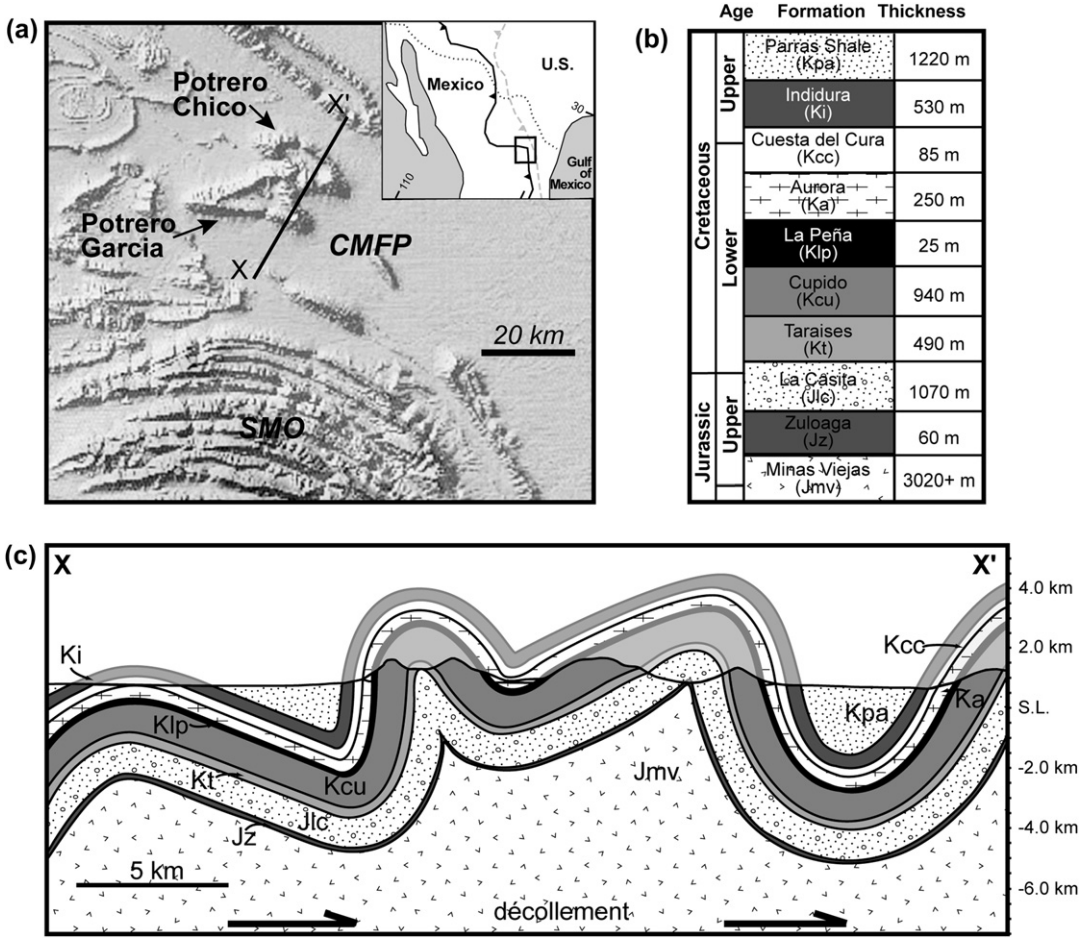

Fig. 1. (a) Index and hill shade maps showing the location of the Sierra del Fraile anticlinorium in the Coahuila Marginal Folded Province (CMFP) in the foreland of the Sierra Madre Oriental fold belt (SMO), northeast Mexico. Inset index map locates the study area with respect to the thin-skinned (solid) and thick-skinned (dashed) deformation fronts. The regional-scale fold consists of two anticlines, Potrero Chico to the north and Potrero Garcia to the south. (b) Stratigraphic column of Mesozoic deposits that outcrop in the Sierra Madre Oriental foreland. Formation thicknesses are based on field measurements and published sections (Goldhammer et al., 1991). (c) Cross section through the Sierra del Fraile anticlinorium drawn perpendicular to the strike of the average fold axes determined from bedding poles throughout the anticlinorium (V = H).

3. Methods

In order to constrain the kinematic history of Sierra del Fraile, the geometry of the anticlinorium was constructed from field mapping (525 km^2 area at a 1:25,000 scale), aerial photographic analysis, and variably oriented cross sections (Latta, 2005) (Fig. 2a). Sierra del Fraile is a domal anticlinorium composed of two doubly plunging anticlines, Potrero Chico to the north and Potrero Garcia to the south. Potrero Chico (~19 km long) has a fold axis that trends NW-SE (Fig. 2b), while the hinge line of Potrero Garcia (~22 km long) curves from a roughly E-W orientation to a roughly

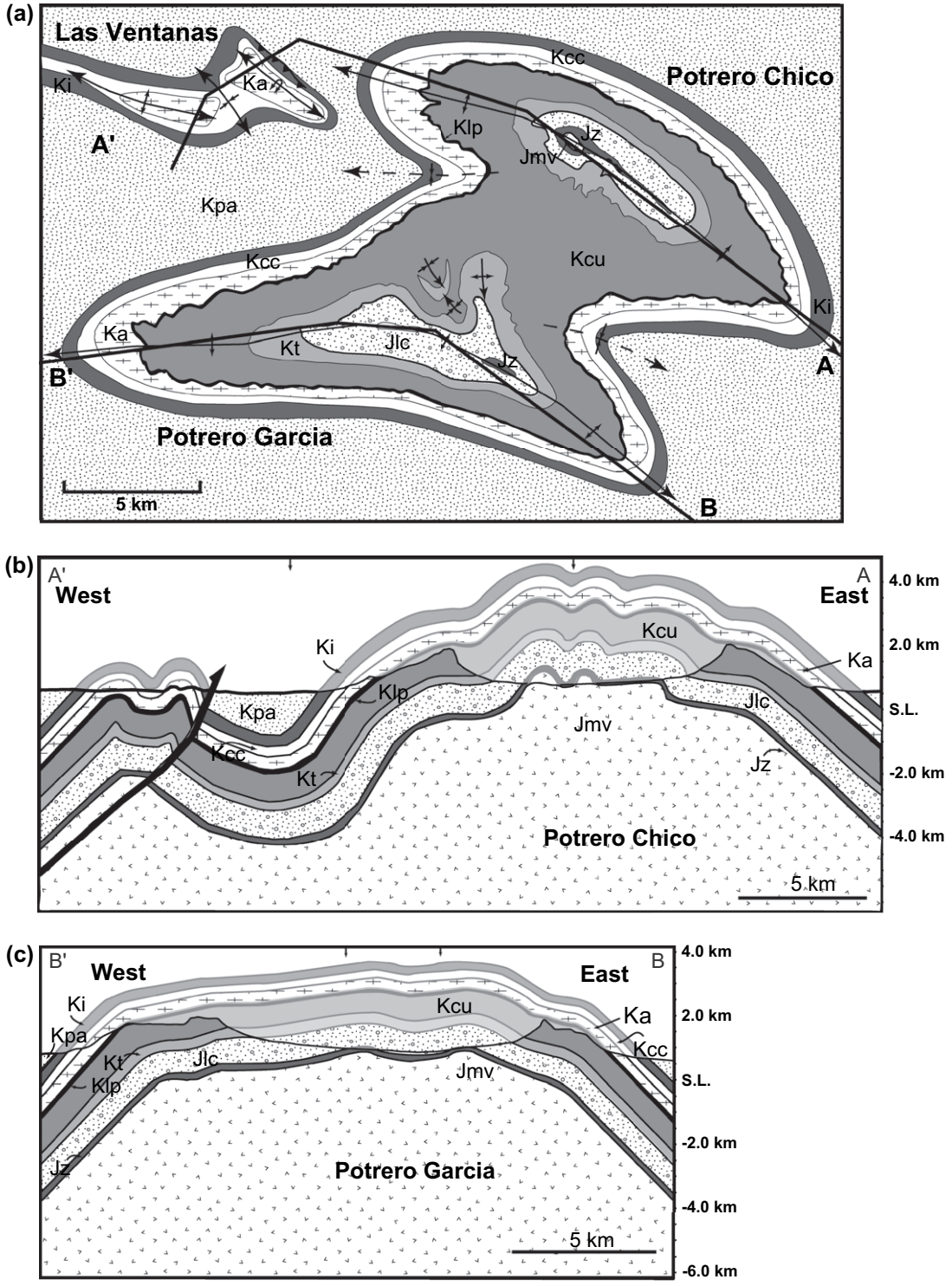

Fig. 2. (a) Simplified geologic map of Sierra del Fraile and Las Ventanas based on 1:25,000 scale field mapping (Latta, 2005). (b) Cross section along the fold axis of Potrero Chico (A–A′). Arrows at the top of the cross section indicate changes in the orientation of the section. (c) Cross section along the fold axis of Potrero Garcia (B–B′). Arrows at the top of the cross section indicate changes in the orientation of the section.

NW-SE orientation to the east (Fig. 2c). The dome plunges 40–50° at both ends, with bedding dipping ~80° on the outer fold limbs. The two anticlines are separated by the Arista syncline to the west and the Escobedo syncline to the east. Cross-sections (Figs. 1c, 2b,c) characterize the regional-scale geometry of the anticlinorium and provide a framework to interpret mesoscopic- and microscopic strain data, which are used to constrain fold kinematics and to define lithotectonic units. Depth-to-detachment calculations assuming equal cross sectional area (Epard and Groshong, 1993) were completed using the massive Cupido Formation as reference (Fig. 1c).

During folding, layered rocks accumulate discrete (flexural slip) or distributed (flexural flow) simple shear, whose magnitude increases with distance from pin lines and bedding dip. Alternatively, folding accommodated by orthogonal flexure results in maximum strains in fold hinges along layer boundaries and minimum strains within the layer and along fold limbs (Ramsay, 1967). During folding, hinges can be pinned or migrating, and characterization of shear sense and magnitude can be used to establish pin positions (Suppe and Namson, 1979; Fischer and Woodward, 1992; Anastasio et al., 1997; Homza and Wallace, 1997; Salvini and Storti, 2004). The location of pin lines and the orientation, distribution, and sense of layer-parallel shear constrains the appropriate fold kinematic model. Mesoscopic structures, including extension and shear fractures, stylolites, and cleavage, were measured in diverse lithologies in both limb and hinge positions and analyzed for sense of shear to locate pin lines. These mesoscopic structures were also used to validate the use of anisotropy of magnetic susceptibility (AMS) as a proxy for penetrative tectonic strain orientations.

The geometry of penetrative strain was determined by measuring the AMS on oriented samples from limb and hinge positions in multiple facies in the thin-bedded shales of the La Casita, La Peña, and Cuesta del Cura Formations, and the thick-bedded carbonates of the Cupido and Taraises Formations. Shale units were preferentially chosen since they are likely to record greater and more uniform strains than other lithologies as AMS is sensitive to phyllosilicate (paramagnetic) grain fabrics (Ramsay and Huber, 1987; Parés and van der Pluijm, 2002). AMS is a measure of the bulk fabric of all magnetic minerals within a rock, where the anisotropy is a function of the preferred mineral orientation (Borradaile, 2001). AMS is described by a second order symmetric tensor analogous to the finite strain tensor and is represented geometrically by an ellipsoid with principal axes $k_{max} \geq k_{int} \geq k_{min}$. AMS axes orientations were demonstrated to show a one-to-one correlation with principal strain directions (i.e. $X = k_{max}$, $Y = k_{int}$, $Z = k_{min}$) (Kligfield et al., 1981; Borradaile, 1991; Borradaile and Henry, 1997). Since carbonates are alloclastic deposits they tend to have less depositional fabric than siliclastic sediments and typically lithify with less compaction, therefore, the susceptibility ellipsoid is dominated by the tectonic strain. This is important in low strain rocks, where depositional and diagenetic fabrics can obscure the tectonic strain. Evans et al. (2001) showed that AMS ellipsoids are sensitive recorders of strain orientation and magnitude in Paleozoic limestones in the central Appalachians, despite the fact that calcite is diamagnetic, and that carbonates consequently often have low or negative magnetic susceptibilities. Likewise, Burmeister et al. (2004) argued that AMS is a better tool for resolving fabric orientations and strain history than Fry or R^f/ϕ methods in the low strained rocks of the Hudson Valley fold and thrust belt, northern Appalachians. In this study, only the orientation of the AMS fabric ellipsoid is considered, since the magnitude of magnetic susceptibility varied between carbonate facies from the same structural position. AMS fabrics were measured on an Agico KLY-3s Kappabridge at Lehigh University.

4. Results

Complexly deformed evaporites of the Minas Viejas Formation outcrop in the anticlinal hinge of Potrero Chico. The overlying limestones of the Zuloaga Formation are exposed in scattered outcrops within the core of both folds and are mesoscopically folded and faulted, exhibiting numerous gypsum veins that vary widely in orientation (Fig. 3, stations 9, 13). Surface deposits blanket much of the area underlain by the La Casita Formation and older units (Fig. 2). Observations from a single outcrop of the La Casita Formation on the northern limb of the anticlinorium indicate a strong bedding fissility in the shale layers. Both joints and veins vary in orientation but most are oriented perpendicular to bedding with moderate to steep (42–78°) dips (Fig. 3, station 8). Cleavage is roughly parallel to bedding. Shear fractures were not observed. AMS fabrics from samples of the La Casita Formation on the north limb of the anticlinorium record an oblate fabric, where $k_{max} \approx k_{int} > k_{min}$. The results further indicate a foliation fabric that is steeply inclined and dipping shallowly away from the axial surface (Table 1, Fig. 4, station 5).

The Taraises Formation consists of interbedded shales and limestones. Mesoscopic deformation features on the limbs of the anticlinorium vary in abundance and orientation in association with changes in lithology and bed-thickness (Fig. 3, stations 6, 7, 12). Deformation patterns in the thin-bedded (0.2–0.5 m thick) limestones and shales of the lower 80% of the unit (~420 m) are distinct from deformation in the thicker-bedded (0.5–1.0 m thick) limestones in the top of the unit (~70 m). The upper and lower portions of the Taraises Formation on each limb are separated by a 1–2 m protocataclasite interval. In the upper portion of the Taraises Formation mesoscopic deformation features are sparse, with only a few bed-perpendicular fractures. In the lower portion of the Taraises Formation, bed-bounded, bed-perpendicular fractures are abundant in the limestone layers, while shales display a strong bed-parallel fissility. Bed-parallel faults in the shale layers indicate a top towards the hinge sense of displacement based on calcite mineral accretion steps in shear fibers. In the northern limb, the minimum shortening direction measured from extension and shear fractures agrees (105°/10°) (Fig. 3, station 6), as do the maximum shortening direction measured from shear fractures and that recorded by the AMS fabric (215°/70°) (Fig. 3, station 6, Fig. 4, station 4). In an outcrop on the south dipping limb of

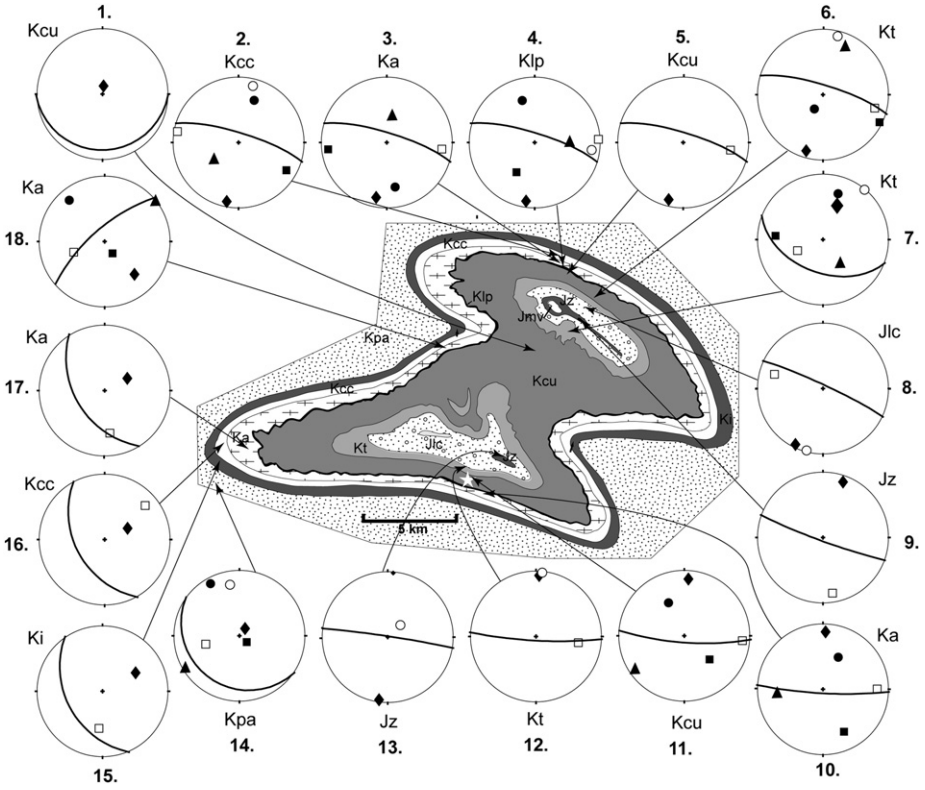

Fig. 3. Summary equal area, lower hemispheric, stereographic projections of principal strain axes. *X* (squares), *Y* (triangles), *Z* (circles) from shear fractures (filled symbols), *X* from extension fractures (open squares), *Z* from cleavage surfaces (open circles), are plotted with average bedding as a great circle and pole to bedding (diamond) throughout Sierra del Fraile. White star indicates study site in the Cupido Formation illustrated in Fig. 6.

Potrero Chico, beds from the lower portion of the Taraises Formation are highly deformed (Fig. 3, station 7). The outcrop contains multiple sets of joints, veins, and shear fractures both parallel and oblique to bedding. Here, a thrust fault and fault-related folds indicate displacement toward the anticlinal hinge of Potrero Chico. In addition to the numerous minor faults and folds, penetrative deformation is heterogeneous at the sub-meter scale. A coarse-grained, ~1.0 m thick unit of bioherm facies has no cleavage, while a finer-grained, 0.5 m thick lagoon bed exhibits moderate to strong cleavage oblique to bedding, and the overlying coarser-grained, shoal unit exhibits weaker disjunctive cleavage perpendicular to bedding (Fig. 5a).

AMS collected from a ~0.5 m thick carbonate layer in the Taraises Formation on the north-dipping limb of the fold indicates an oblate fabric with the flattening plane oriented oblique to bedding and moderately inclined towards the axial surface (Table 1, Fig. 4, station 4). AMS in samples collected from the southern limb of Potrero Chico records an oblate fabric oriented nearly parallel to bedding or moderately steeper, indicating a top towards the anticlinal hinge sense of shear (Table 1, Fig. 4, station 7).

The massively-bedded carbonates of the Cupido Formation contain few mesoscopic deformation features (Fig. 3, stations 1, 5, 11). Bed-parallel stylolites are scattered throughout the unit and are preferentially located at the interface between coarser and finer-grained facies (e.g. between bioherm and lagoon, and shoal and tidal flat facies). Stylolites near the base of the formation in Potrero Garcia indicate varying degrees of shear towards the anticlinal hinge (Fig. 6). Extension fractures also indicate strong facies control within the upward shallowing, meter-scale carbonate cycles that characterize the formation. Extensional fractures tend to be localized in coarser-grained, carbonate-rich shoal and build up facies, where they are often bed bounded within the 1–2 m thick layers. Most fractures are perpendicular to bedding and fracture spacing varies with bed thickness, where wider spaced fractures are preferentially located in the thicker beds (Fig. 3, stations 5, 11). Sparse bed-parallel faults are found near the base of the formation on the southern limb (Fig. 3, station 11). At the top of the unit, brittle-ductile shear zones cross cut bed-parallel stylolites and some bed-perpendicular fractures indicate a right-lateral sense of shear. On the south dipping limb, faults at the base of the unit indicates hingeward shear (Fig. 3, station 11).

The lower Cupido Formation is exposed in the hinge of the Sierra del Fraile anticlinorium (Fig. 3, station 1). The shallow-dipping (~10°) beds of the Cupido Formation represent the uppermost unit exposed in the hinge and contain few mesoscopic deformation features. The steepness of the exposure limits our observations to a narrow stratigraphic interval where rare, bed-perpendicular joints are bed-bounded in the coarser-grained shoal and build-up facies, but no bed-parallel stylolites or faults, or other mesoscopic evidence of penetrative shear were observed.

AMS in the Cupido Formation was measured in samples from both limb and hinge positions where each records an

Table 1
Bedding (S,D,DD) and AMS (T,P) orientations in geographic coordinates for samples collected from both carbonate and clastic units at Sierra del Fraile

	Bedding	k_{max}	k_{int}	k_{min}
La Casita	295/85 N	227/64	117/10	023/24
	295/85 N	272/56	107/33	013/07
	295/85 N	291/35	097/54	196/07
	295/85 N	274/14	155/64	010/22
Taraises	287/78 N	311/16	141/74	042/03
	287/78 N	231/68	141/00	051/22
	111/48 S	329/16	183/71	062/10
	111/48 S	330/27	217/36	087/42
	111/48 S	208/71	168/14	075/11
Cupido	285/80 N	137/64	010/16	274/19
	285/80 N	162/67	018/19	284/13
	285/80 N	108/61	000/10	264/27
	285/80 N	104/25	194/01	286/65
	285/80 N	050/53	199/33	299/15
	285/80 N	079/31	343/09	239/57
	285/80 N	168/68	039/14	305/16
	094/77 S	139/35	035/20	281/49
	094/77 S	298/77	073/09	164/09
	094/77 S	193/66	329/17	064/15
	094/77 S	062/54	215/33	314/13
	094/77 S	143/35	356/50	245/17
	094/77 S	130/63	032/04	300/27
	094/77 S	201/61	068/21	331/20
	090/10 S	344/52	150/37	245/07
	090/10 S	303/11	033/02	135/79
	090/10 S	266/44	144/29	034/33
	090/10 S	331/18	232/26	092/58
	090/10 S	246/04	148/63	339/27
La Peña	278/78 N	112/21	017/12	260/66
Aurora	229/68 N	284/13	020/24	168/03
Cuesta	281/83 N	303/05	184/80	033/09
del Cura	281/83 N	279/74	108/16	018/03
	281/83 N	245/72	084/17	352/05
	281/83 N	294/45	066/34	175/26
	152/43 W	232/41	326/05	061/48
Indidura	150/40 W	210/52	323/17	064/33
	150/40 W	224/08	316/13	103/75

oblate fabric (Fig. 4, stations 3, 7, 11). Limb samples contain foliation perpendicular to bedding (Table 1, Fig. 6). Near the hinge, AMS samples each record flattening planes parallel to bedding with k_{min} axes nearly perpendicular to bedding. On the south dipping limb, AMS agrees with principal strain axes determined from populations of shear fractures with k_{max} oriented 171°/21°, k_{int} oriented 273°/29° and k_{min} oriented 051°/53° (Fig. 6). Here, fabric orientations in the Cupido Formation are consistent with up-dip shear to the northeast, coincident with shear toward the nearby anticlinal hinge.

To test for facies based control on strain heterogeneity, deformation was measured in closely spaced samples across a shear zone near the base of the Cupido Formation on the south dipping limb of the anticlinorium (Fig. 6). The bed-parallel shear zone is within a larger 60 m measured interval in the Cupido Formation where sheared stylolites are observed to be preferentially located in the coarser-grained, thick-bedded (0.4–1.0 m thick) carbonate-rich build-up and shoal facies, whereas bed-parallel faults are located in the thin-bedded (0.1–0.3 m thick), more argillaceous lagoon facies (Fig. 5a). Here mesoscopic strain indicators exhibit a clear partitioning of discrete and penetrative strain as a function of facies-based differences in competency and anisotropy between beds. Originally perpendicular teeth of bed-parallel stylolites in coarser-grained, carbonate-rich (i.e. more competent), thick-bedded (i.e. less anisotropic) shoal and build up facies record a mean rotation of −2 to −24° to the north, consistent with layer-parallel shear towards the fold hinge. AMS fabrics on the southern limb of Sierra del Fraile mimic the kinematic patterns of mesoscopic deformation features. The finer-grained, less competent and thin-bedded, more anisotropic lagoon facies, which are bounded by discrete bed-parallel faults, record AMS compaction fabrics. In contrast, rocks in a penetrative shear zone where stylolite fabrics record a maximum of −36° rotation to the north, AMS principal axes correspond well with the distribution and direction of shear (Fig. 6b).

Like the Cupido Formation, the La Peña Formation exhibits rare deformation features. The 0.05–0.4 m thick shale beds occasionally contain closely spaced bed-perpendicular fractures in the more carbonate-rich layers towards the base of the formation, where the principal shortening direction determined from fractures is oriented 087°/01° (Fig. 3, station 4). The unit also contains scattered bed-parallel stylolites. A small amount of bed-parallel shear is recorded by rare faults in the thinner-bedded layers, where calcite shear fibers indicate a top towards the anticlinal hinge sense of displacement (Fig. 3, station 4). The AMS fabric in the La Peña Formation is oblate with a flattening plane parallel to cleavage and perpendicular to bedding (Table 1, Fig. 4, station 1).

Similar to the Cupido Formation and the La Peña Formation, mesoscopic deformation features in the thick-bedded (0.5–1.5 m) carbonates of the Aurora Formation are sparse (Fig. 3, stations 3, 10, 17). Bed-parallel shear fractures on the north and south dipping limbs each record hingeward shear while bed-perpendicular faults display both right- and left-lateral offsets (Fig. 3, stations 3, 10). Shear fractures along the north-dipping limb of the Arista syncline are also consistent with hingeward shear (Fig. 3, station 18). Isolated brittle-ductile shear zones near the base of the formation indicate a top towards the anticlinal hinge sense of shear. Bed-parallel stylolites are less abundant in this unit as compared to the Cupido Formation, as facies transitions are fewer.

Similar to the lower Taraises Formation, the shale and limestone layers (0.2–0.4 m thick) of the Cuesta del Cura Formation contain abundant mesoscopic deformation. Shale layers have pervasive fissility at a shallow angle to bedding (Fig. 3, station 2). In addition, there are numerous bed-parallel faults that display dip-slip motion. In the thicker-bedded limestone layers, bed-perpendicular fractures are numerous and indicate a left-lateral (east side to the north) sense of displacement (Fig. 3, station 2). The Cuesta del Cura Formation also contains minor kink folds. AMS data from the Cuesta del Cura Formation records an oblate fabric parallel to bedding (Table 1, Fig. 4, station 2). Samples collected from fissile shale units (0.1–0.2 m thick beds) record foliation inclined 0–18° from

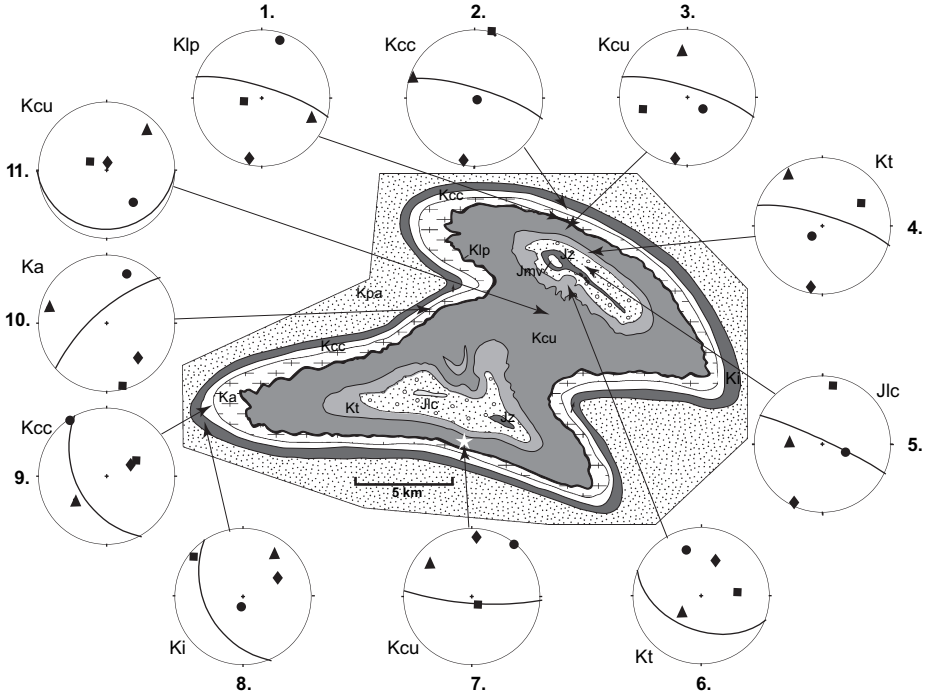

Fig. 4. Summary equal area, lower hemispheric, stereographic projections of principal axes [k_{max} (squares), k_{int} (triangles), k_{min} (circles)] from AMS, are plotted with average bedding as a great circle and pole to bedding (diamond) throughout Sierra del Fraile. White star indicates study site in the Cupido Formation illustrated in Fig. 6.

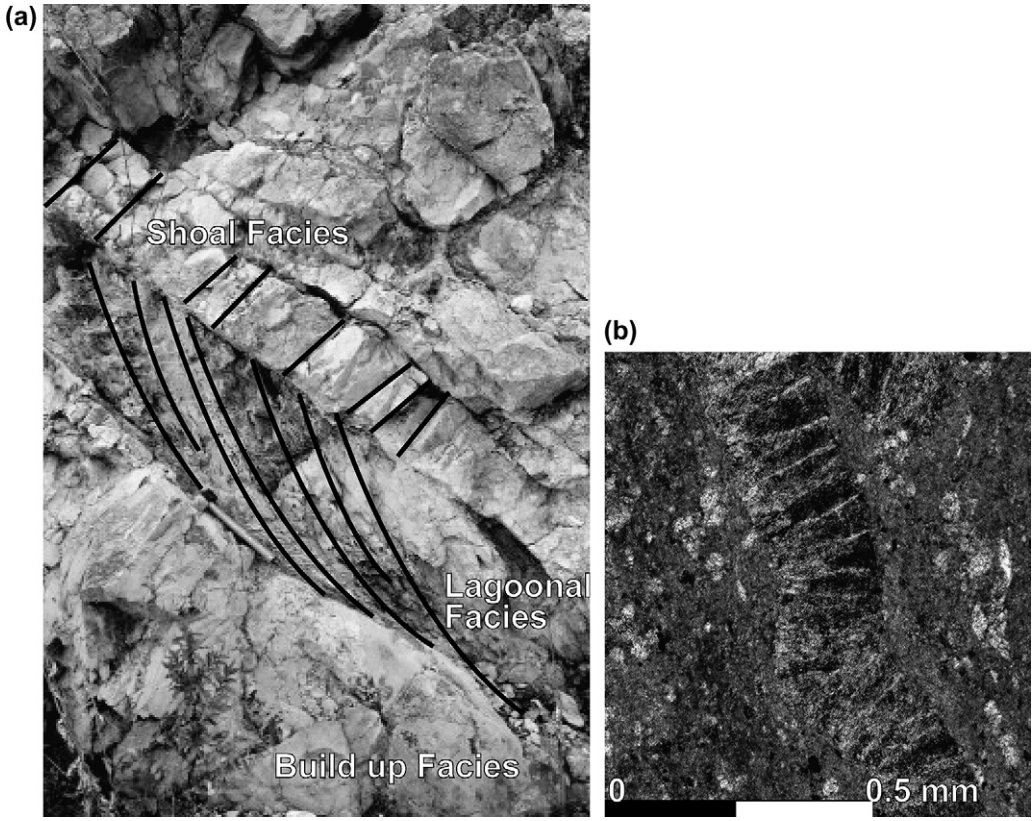

Fig. 5. Strain heterogeneity is observed on a variety of scales. (a) Meter-scale: lagoonal facies of the Taraises Formation displays cleavage (highlighted by black lines), build-up facies show no cleavage and the shoal facies has developed weak disjunctive cleavage (black lines). Rock hammer for scale. (b) Millimeter-scale: Indidura Formation, sub-millimeter thick chert stringers display bed-perpendicular fractures that truncate against the less competent carbonate layers where deformation is dominated by pressure solution.

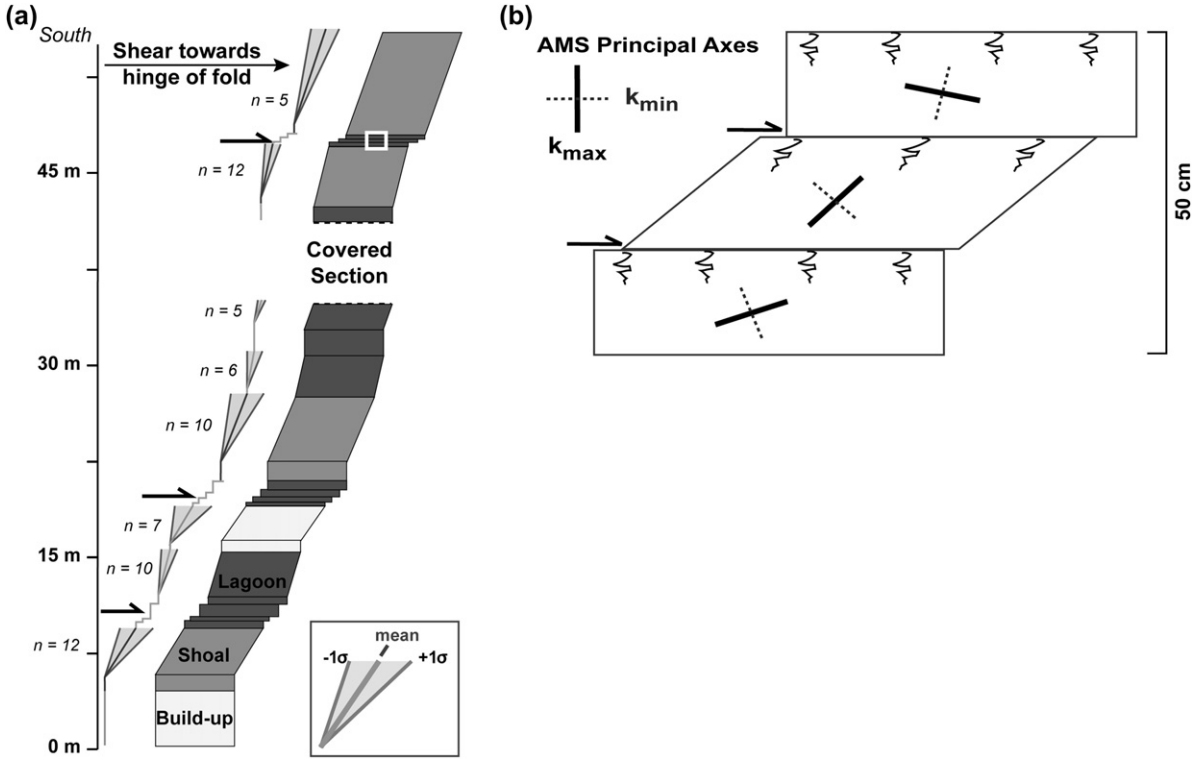

Fig. 6. Distribution of discrete and penetrative strain in a section of the Cupido Formation Bedding dips ~80° to the south. (a) Populations of sheared stylolite teeth shown as a mean and standard deviation from bedding and discrete bed parallel faults (white star Figs. 3 and 4). (b) AMS measurements within a discrete shear zone (white box near top of column in (a)). Strain heterogeneity is observed at fine scales in layers that display shear and unsheared stylolites (crooked lines at layer tops) where AMS records a compaction fabric.

bedding while thicker-bedded (0.3–0.4 m thick) more carbonate-rich units contain a foliation that is more steeply inclined at ~25°, from bedding. At a regional-scale, foliation forms a divergent fan about the anticlinorium. The orientations of principal extension from both fractures and from AMS fabrics on the western plunging end of Potrero Garcia are consistent at 061°/48° (Fig. 4, station 9). In contrast, AMS fabrics collected from the north-dipping limb ($k_{max} = 015°/03°$, $k_{int} = 285°/05°$, $k_{min} = 109°/85°$) are inconsistent with mesoscale fabrics (Fig. 4, station 2).

Isolated outcrops of the Indidura Formation, exposed along the western plunging hinge area of Potrero Garcia, display deformation patterns similar to the Cuesta del Cura and the lower Taraises Formations. The 0.4–0.7 m thick limestone layers display bed-perpendicular joints, while the 0.2–0.3 m thick shale beds display some evidence of bed-parallel shear (Fig. 3, station 15). Poor preservation of shear surfaces prevents identification of the sense of slip. AMS is inconsistent with mesoscale fabrics where k_{max} is oriented 307°/05°, k_{int} is oriented 039°/16° and k_{min} is oriented 199°/74° (Fig. 4, station 8).

The shales of the Parras Formation, which are exposed in isolated outcrops along the limbs of Sierra del Fraile, record more deformation than underlying units. The thin (0.05–0.3 m) layers display pervasive pencil cleavage and minor folds, making identification of bedding surfaces difficult (Fig. 3, station 14). In some cases, cleavage is steep to bedding, but orientations vary within and between outcrops. There are also numerous bed-parallel faults within the shale layers that display variable slip (Fig. 3, station 14). The mean principal shortening direction from cleavage and the principal extension direction from minor faults are parallel to one another and nearly horizontal. Infrequent sandstone units exhibit bed-perpendicular fractures.

5. Discussion

5.1. Mechanical stratigraphy at multiple scales

Differences in the orientation and abundance of deformation features between various lithologies highlight how relative differences in carbonate content, bed thickness and grain size affect rock competency and how changes in bed thickness and argillaceous content associated with carbonate facies controls mechanical anisotropy. At the largest-scale, Sierra del Fraile can best be described as two mechanical units consisting of the 4.5 km thick stiff upper layer of the Jurassic and Lower Cretaceous limestones and clastics over a >3 km thick section of ductile evaporites of the Minas Viejas Formation. It is the ratio of these two layers that controls the décollement position and fold amplitude for a given amount of shortening (e.g. Wiltschko and Chapple, 1977). The Minas Viejas Formation accumulates in rising anticlines and evacuates from beneath sinking synclines, thereby controlling the

distribution of doubly-plunging structural ridges and valleys across the Mexican foreland. Our analysis of the distribution and orientation of mesoscopic deformation from the 10 map units from around one such anticlinorium permits delineation of five regional-scale lithotectonic units, hundreds of meters to kilometers thick that display lithologic and deformation similarities (Table 2).

Lithotectonic unit 1, the lowermost unit, consists of the incompetent, isotropic evaporites of the Minas Viejas Formation (Fig. 1b). This unit, which is widely distributed throughout the foldbelt, is locally >3 km thick, and is classified as its own lithotectonic unit, exhibiting disharmony with overlying carbonates and clastics. The Minas Viejas Formation outcrops in Potrero Chico, but is absent in Potrero Garcia. Beds in the overlying Zuloaga Formation do not exhibit thinning or upturned beds, unconformities between beds or changes in facies away from the salt, suggesting the evaporites were relatively stable during deposition of the limestone units. Additionally, the overlying units lack evidence for crestal extension or vertical shortening suggesting that diapirism did not play a large role during fold formation (e.g. Schwerdtner, 1990).

An increase in the competency and anisotropy of the thin-bedded shales and limestones of the Zuloaga, La Casita and lower 80% of the Taraises Formation, comprise lithotectonic unit 2 (Fig. 1b). Bed-perpendicular joints in these formations display similar patterns in the orientation and abundance with bed-bounded joints in the more competent limestone layers and bed-parallel shear fractures in the less competent, highly anisotropic shale layers, which possess a strong bedding fissility (Table 2). The inclusion of the lower portion of the Taraises Formation in lithotectonic unit 2 is important in that it signifies that lithotectonic units need not be coincident with stratigraphic formations, which tend to be based on lithology and outcropping characteristics.

Lithotectonic unit 3 is the most competent unit. Mesoscopic deformation features are sparse within lithotectonic unit 3, which consists of the platform carbonates of the Cupido and Aurora Formations, the intervening shales of the La Peña Formation, and the upper 20% of the Taraises Formation (Fig. 1b). It is important to note, that even though the La Peña Formation is by itself incompetent and anisotropic, it behaves similarly to the surrounding competent, thick-bedded carbonates of the Cupido and Aurora Formations. Deformation features in lithotectonic unit 3 consist mostly of bed-perpendicular joints and veins, and occasional bed-parallel faults, which are located near the upper and lower formation contacts within and near the thinner-bedded facies (Table 2). Lithotectonic unit 3 is the only mechanical unit that displays bed-parallel stylolites. This unit is the dominant fold member exhibiting the largest fold wavelength. The contact between lithotectonic units 2 and 3 is based on a brittle deformation zone in the upper Taraises Formation on fold limbs. On each limb, layers below a protocataclasite interval contain more joints, veins, and shear fractures, while layers above contain fewer fractures. A change in the stratigraphic position of the boundary between lithotectonic units 2 and 3 on the north

Table 2
The distribution and orientation of mesoscopic deformation features in Sierra del Fraile

Formation	Lithotectoni unit									
	1	2			3			4		5
	Minas Viejas	Zuloaga	La Casita	Taraises	Cupido	La Peña	Aurora	Cuesta del Cura	Indidura	Parras
Rock type	Evaporites	Limestones	Limestones shales	Limestones shales	Limestones	Shales	Limestones	Limestones shales	Limestones shales	Shales
Bed thickness	n/a	Thin to thick 0.2–0.5 m	Thin to thick 0.2–0.5 m	Thin to thick 0.2–1.0 m	Thick 1.0–2.0 m	Thin 0.05–0.4 m	Thick 0.5–1.5 m	Thin to thick 0.2–0.4 m	Thin to thick 0.2–0.7 m	Thin 0.05–0.3 m
Deformation features	n/a	Abundant	Abundant	Abundant	Sparse	Moderate	Sparse	Abundant	Moderate	Abundant
Extensional fractures	n/a	bed ⊥, bed ∥	bed ⊥, bed ∥	bed ⊥, bed ∥	bed ⊥, rare bed ∥	bed ⊥, bed ∥	bed ⊥, rare bed ∥	bed ⊥, bed ∥	bed ⊥, bed ∥	bed ⊥, bed ∥
Shear fractures	n/a	Bed ∥	Bed ∥	Bed ∥	Bed ⊥, rare bed ∥	Bed ∥	Bed ⊥, rare bed ∥	Bed ⊥, bed ∥	Bed ∥	Bed ∥
Minor folds	n/a	No	No	No	No	No	No	m-dm scale asymmetric kink folds	No	m-dm scale
Cleavage	n/a	No	No	No	No	No	No	Moderate to strong	No	Strong
AMS	n/a	n/a	Compaction LPS	Compaction late flattening	Compaction LPS	Compaction late flattening	LPS	Compaction LPS	Compaction	Compaction

The differences in the orientation and abundance of deformation features between the units helped to define the regional-scale mechanical stratigraphy. (⊥, approximately perpendicular; ∥, approximately parallel).

and south dipping limbs, respectively, is associated with a facies change to more carbonate rich, thicker beds at this stratigraphic interval between outcrops that palinspastically restore to ~25 km apart.

Lithotectonic unit 4 contains prevalent bed-parallel faults in shale layers and bed-perpendicular shear fractures in the limestone layers. Unit 4 consists of a succession of relatively incompetent and more anisotropic, thin- to thick bedded, limestones and shales of the Cuesta del Cura and Indidura Formations (Fig. 1b). The abundance of bed-parallel cleavage within the Cuesta del Cura Formation helps to distinguish this mechanical unit from lithotectonic unit 3 (Table 2). Unit 4 is also distinct because of the disharmonic decameter- to meter-scale kink folds in the Cuesta del Cura Formation.

The uppermost mechanical unit in Sierra del Fraile, lithotectonic unit 5, displays the greatest abundance of deformation including minor folds, multiple bed-parallel faults and pervasive pencil cleavage throughout the unit (Table 2). The observed disagreement between penetrative strain and shortening direction determined by discontinuous fabrics may result from strain heterogeneities or shifting strain direction through time (e.g. Beach, 1982). Unit 5 consists of a thick succession of mudstones within the incompetent Parras Formation (Fig. 1b).

Although five lithotectonic units comprise the mechanical stratification of Sierra del Fraile at a regional-scale, observations in outcrop and petrographically indicate stratigraphic control on strain heterogeneity at smaller scales as well (Fig. 5). On the south dipping limb of the fold, strain is partitioned at the meter-scale in the Cupido Formation with discrete bed-parallel shear in thin-bedded, fine-grained, less competent, more anisotropic lagoon facies and penetrative shear in the thicker-bedded, coarser-grained, more competent, and less anisotropic shoal and build-up facies (Fig. 5a). Similarly, on the southern limb of Potrero Chico, the Taraises Formation displays cleavage in the thin-bedded, finer-grained, more argillaceous, less competent and more anisotropic lagoon facies, whereas cleavage is absent in the thicker-bedded, coarser-grained, more competent, less anisotropic shoal and build-up facies that surround it (Fig. 5a).

In the Sierra Madre Oriental fold belt, Fischer and Jackson (1999) used the distribution of deformation to define six lithotectonic units above the Minas Viejas Formation along the northern limb of Nuncios fold. The mechanical units were divided along formation boundaries and further subdivided based on the distribution and orientation of strain features into smaller-scale mechanical units. The study focused on a single structural position and found that deformation patterns vary widely across the stratigraphic succession. Our results agree with the findings of Fischer and Jackson (1999) that deformation patterns vary within the Mesozoic section and furthermore allow the following generalizations. Thin-bedded units have better developed cleavage and more layer-parallel shear fractures. Thicker-bedded carbonate rich units develop bed-bounded joints and veins, generally at a high angle to bedding. Agreement between AMS and mesoscale strain orientations is found more often in thin-bedded, finer-grained units that have better developed cleavage and layer-parallel faults than in thicker-bedded coarser units that contain sparse mesoscopic deformation, and a higher percentage of carbonate.

Because deformation patterns vary with stratigraphy and folding, reservoir properties are likewise expected to vary with facies and deformation history. Our field observations allow us to make the following generalizations. In the finer-grained lagoon beds, where cleavage is more prominent, porosity-based permeability will decrease with decreasing grain size and increasing strain by diffusion creep. In shoal and build up facies, the coarser-grained facies will have an inherently higher porosity and throughgoing fractures will increase permeability, while in regions of intense cataclastic flow both porosity and permeability, and thus reservoir quality will decrease (e.g. Mitra, 1987). By characterizing the distribution and orientations of deformation features at multiple structural positions, we determined fold kinematics with the characterization of lithotectonic units.

5.2. Fold kinematics

AMS measurements in the La Casita, Cupido and Cuesta del Cura Formations on the north limb, the Cupido Formation on the south limb, and the Aurora Formation on the north dipping limb of the Arista syncline all record fabric orientations consistent with early layer parallel shortening (Table 1, Fig. 4). These fabrics are similar to prefolding layer-parallel fabrics observed in the Appalachian Valley and Ridge and Plateau Provinces (Nickelsen, 1979; Geiser and Engelder, 1982; Gray and Mitra, 1999), and the Umbre-Marche Apennines (Tavarnelli, 1999). However, in the Mexican foreland, as compared to the Appalachian and Apennine carbonate thrust sheets, pressure solution strain has not produced visible cleavage. The cleavage front in the Spanish Pyrenees is coincident with a principal shortening from pressure solution strain of >5% at temperatures of >195°C (Holl and Anastasio, 1995), which are hotter than estimates from the Mexican foreland (Gray et al., 2001). AMS fabrics in the Taraises, Cupido, La Peña and Aurora Formations agree with strain directions inferred from discontinuous brittle features, suggesting strain is homogeneous and that AMS is a sensitive recorder of low temperature penetrative strain in these competent limestones and less competent argillaceous limestones and shales. Additionally, AMS and mesoscale fabric orientations agree in the Taraises and La Peña Formations on the north limb, and indicate late fold flattening. Likewise, mesoscopic deformation features from the La Casita, Cupido, and Aurora Formations on the north limb, and the Taraises, Cupido, and Aurora Formation on the south limb are consistent with late flattening.

The presence of bed-parallel faults, sheared stylolites, and AMS data from the lower Cupido Formation, indicate that following early layer-parallel shortening, lithotectonic unit 3 deformed by a combination of flexural-slip and orthogonal flexure, with discrete bed-parallel slip concentrated along bedding surfaces in the less competent, more anisotropic facies (Fig. 7c). Similarly, mesoscopic deformation features in lithotectonic units 2 and 4 indicate discrete strain partitioning along

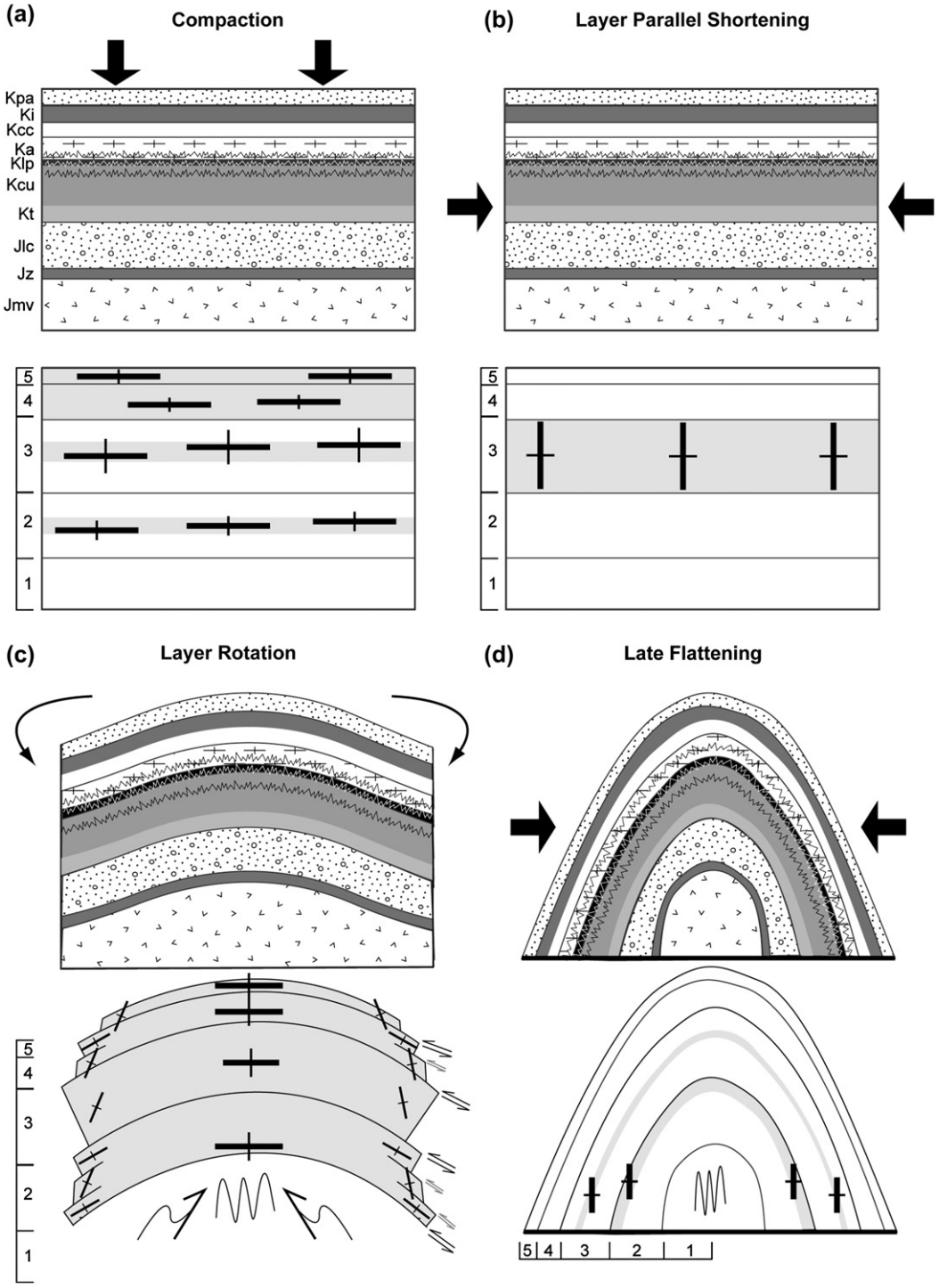

Fig. 7. Deformation history of the Mexican section (top blocks) and the corresponding strain history in the 5 lithotectonic units (lower blocks). (A) Pre-tectonic compaction is followed by (B) layer-parallel shortening and then (C) buckling and finally (D) late flattening.

numerous bedding planes during folding (Fig. 7c). There is evidence at both the mesoscopic and microscopic scale of late fold flattening (Fig. 7d). This is not surprising given the overall tightness of the anticlinorium. Flexural processes are progressively inefficient in fold tightening and shortening as limbs steepen beyond 45° dips (Ramsay, 1967; Woodward, 1997; Fischer and Jackson, 1999).

In Sierra del Fraile, the superposition of mesoscopic structures suggests evolving kinematics during folding (e.g. Gray and Mitra, 1999; Tavarnelli, 1999) (Fig. 7). Less competent, more anisotropic lithotectonic units 2, 4, and 5 experienced compaction then flexural-slip folding, while the more competent, less anisotropic lithotectonic unit 3 was first compacted to generate bed-parallel stylolites, then

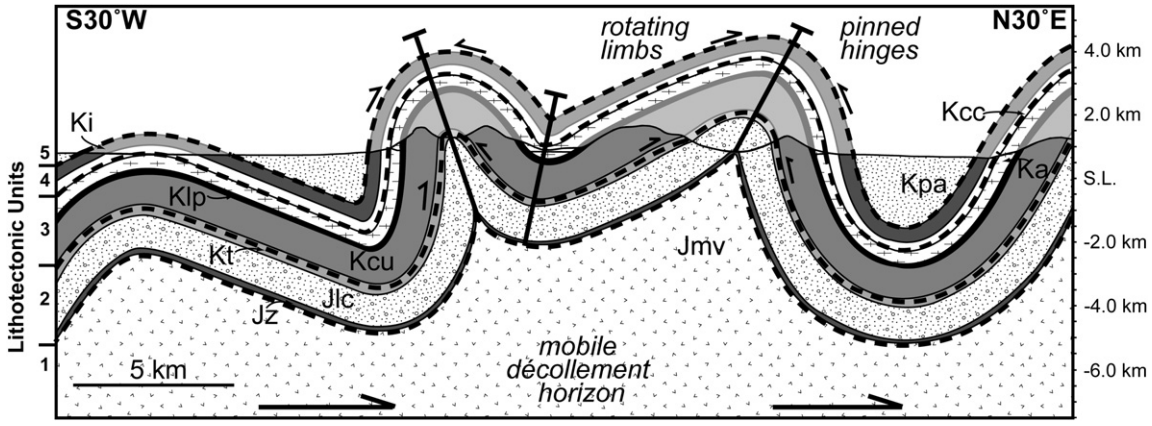

Fig. 8. Sierra del Fraile kinematics and lithotectonic units (separated by bold dashed lines) of the Mexican foreland.

deformed by layer-parallel shortening, and finally folded by a combination of flexural-slip and orthogonal flexure. At the largest-scale, hingeward shear on opposing fold limbs constrains pin lines at fold hinges (Ramsay, 1967) (Fig. 8). A pinned anticline and syncline fold hinge argues for constant limb length and requires a variable décollement horizon within the Minas Viejas evaporites (Homza and Wallace, 1995, 1997). Depth-to-detachment calculations from Fig. 1c suggest basal décollement depths in the Minas Viejas Formation could have varied between ~7 km and ~4 km across the Coahuila Marginal Folded Province.

Deformation patterns within the five lithotectonic units indicate multiple detachment horizons during folding. In addition to the regional décollement in the Minas Viejas Formation, a greater amount of shortening in lithotectonic 5 than unit 4 indicates a décollement horizon in the Parras Formation; a previously recognized décollement horizon in the Coahuila Marginal Folded Province (Wilson, 1999; Higuera-Diaz et al., 2005). Similarly, the strong discordance between mesoscopic deformation patterns in lithotectonic units 2 and 3 supports a décollement horizon at the boundary between these units. This décollement is at a different stratigraphic level in the Taraises Formation on each limb, due to stratigraphic differences on the preorogenic platform. In each case the décollement is located at the transition from the finer-grained, thinner-bedded, deeper-water limestones and shales, to the coarser-grained, thicker-bedded, shallower-water limestones.

At Sierra del Fraile, individual shallowing upward carbonate cycles show variations in anisotropy and competency (Fig. 9). A lack of penetrative strain with an abundance of extension fractures dominate in massively bedded build up facies, while bedding-parallel faults and penetrative strain as measured by AMS dominates in both shallow and deeper water facies (i.e. lagoonal, shoal, basinal, etc.). This partitioning of discrete and penetrative strain varies regularly as a function of facies, which in platform carbonates are controlled by changes in water depth.

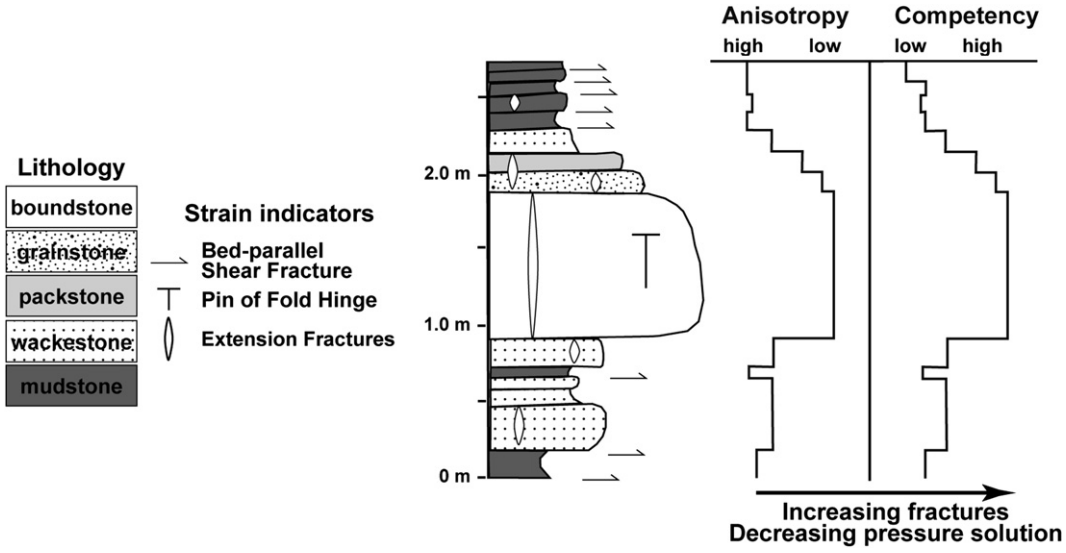

Fig. 9. Individual shallowing upward carbonate cycles show both variations in anisotropy and competency as a function of lithology and bed thickness. This pattern of discrete and penetrative strain varies regularly as a function of facies.

6. Conclusions

Stratigraphy in the Sierra del Fraile décollement fold in northeast Mexico controlled the partitioning of discrete and penetrative strain, as well as fold kinematics. Differences in competency and anisotropy of the carbonate section, largely influenced by variations in detrital content and bedding thickness, resulted in characteristic patterns of deformation at the regional to outcrop scales. Décollement folding occurred by limb rotation about fixed anticlinal and synclinal hinges, with a mobile décollement horizon in the ductile evaporites that core the anticlinorium. Deformation patterns allow for the delineation of five lithotectonic units. The orientations of AMS fabrics and mesoscopic deformation features generally agree with one another and suggest that following initial compactive stylolites in lithotectonic unit 3, several beds were subjected to layer-parallel shortening. Continued shortening resulted in flexural slip folding in lithotectonic units 2, 4, and 5 and a combination of flexural-slip and orthogonal flexure in lithotectonic 3, the stiffest member. Variations in orientation and abundances of deformation features between the lithotectonic units suggest regional décollement horizons in the upper Taraises Formation between lithotectonic units 2 and 3, and the shales of the Parras Formation between lithotectonic units 4 and 5, as well as in between lithotectonic units 1 and 2. The ability to predict deformation behavior and thus fold kinematics in lithotectonic units allows for the prediction of reservoir properties within the anticlinorium and by analogy across an orogen.

Acknowledgments

We thank N.W. Harkins for field assistance, K. Kodama for use of his paleomagnetic lab at Lehigh University and discussion of AMS results, R. Allmendinger for use of his structural software, and L. Tauxe for use of her software to average AMS tensors. This study was supported by Collaborative National Science Foundation grant EAR-0230053 to Anastasio, Kodama, and Elrick, and graduate student research grants from the Geological Society of America, AAPG, and Sigma Xi to Latta. This paper represents a portion of DKL's PhD dissertation at Lehigh University. We thank M. Fischer for his review, which clarified the manuscript.

References

Anastasio, D.J., Fisher, D.M., Messina, T.A., Holl, J.E., 1997. Kinematics of décollement folding in the Lost River Range, Idaho. Journal of Structural Geology 19, 355–368.

Beach, A., 1982. Chemical processes in deformation at low grades: pressure solution and hydraulic fracturing. Episodes 4, 22–25.

Biot, M.A., 1964. Theory of folding stratified viscoelastic media and its implications in tectonics and orogenesis. Geological Society of America Bulletin 72, 1595–1620.

Borradaile, G.J., 1991. Correlation of strain with anisotropy of magnetic susceptibility (AMS). Pure Applied Geophysics 135, 15–29.

Borradaile, G.J., 2001. Magnetic fabrics and petrofabrics: their orientation distributions and anisotropies. Journal of Structural Geology 23, 1581–1596.

Borradaile, G.J., Henry, B., 1997. Tectonic applications of magnetic susceptibility and its anisotropy. Earth Science Reviews 42, 49–93.

Burmeister, K.C., Bannister, R.A., Marshak, S., Ferre, E.C., 2004. Comparison of AMS and strain-analysis results: resolving shortening directions in low-strain rocks of a fold-thrust belt. Geological Society of America Abstracts with Programs 36, 434.

Currie, J.B., Patnode, A.W., Trump, R.P., 1962. Development of folds in sedimentary strata. Geological Society of America Bulletin 73, 655–674.

Dahlstrom, C.D.A., 1969. The upper detachment in concentric folding. Canadian Petroleum Geologist Bulletin 17, 326–346.

Dahlstrom, C.D.A., 1990. Geometric constraints derived from the law of conservation of volume and applied to evolutionary models for detachment folding. American Association of Petroleum Geologists Bulletin 74, 336–344.

Davis, D.M., Engelder, T., 1985. The role of salt in fold-and-thrust belts. Tectonophysics 119, 67–88.

Dennis, J.G., 1967. International Tectonic Dictionary. American Association of Petroleum Geologists Memoir 7.

De Sitter, L.V., 1956. Structural Geology. McGraw-Hill, New York.

Dickinson, W.R., Lawton, T.F., 2001. Carboniferous to Cretaceous assembly and fragmentation of Mexico. Geological Society of America Bulletin 113, 1142–1160.

Dixon, J.M., 2004. Physical (centrifuge) modeling of fold-thrust shortening across carbonate bank margins - timing, vergence, style of deformation. In: McClay, K.R. (Ed.), Thrust Tectonics and Hydrocarbon Systems. American Association of Petroleum Geologists Memoir 82, pp. 223–238.

Donath, F.A., 1962. Role of layering in geological deformations. New York Academy of Science Transactions 24, 236–249.

Donath, F.A., 1969. The development of kink bands in brittle anisotropic rocks. Geological Society of America Memoir 115, 453–493.

Donath, F.A., Parker, R.B., 1964. Folds and folding. Geological Society of America Bulletin 75, 45–62.

Elliott, D., 1981. Balanced cross sections, the methods and programs: stage I. Unpublished notes, Baltimore, MD.

Epard, J.L., Groshong, R.H., 1993. Excess area and depth to detachment. American Association of Petroleum Geologists Bulletin 77, 1291–1302.

Epard, J.L., Groshong, R.H., 1995. Kinematic model of detachment folding including limb rotation, fixed hinges and layer-parallel strain. Tectonophysics 247, 85–103.

Evans, M.A., Lewchuk, M., Elmore, D.R., 2001. Strain partitioning of deformation mechanisms in limestones: examining the relationship of strain and anisotropy of magnetic susceptibility (AMS). Geological Society of America, 2001 Annual Meeting Abstracts with Programs. Geological Society of America 33, p. A149.

Fischer, M.P., Jackson, P.B., 1999. Stratigraphic controls on deformation patterns in fault-related folds: a detachment fold example from the Sierra Madre Oriental, northeast Mexico. Journal of Structural Geology 21, 613–633.

Fischer, M.P., Woodward, N.B., 1992. The geometric evolution of foreland thrust systems. In: McClay, K.R. (Ed.), Thrust Tectonics. Chapman and Hall, London, pp. 181–189.

Fisher, D.M., Anastasio, D.J., 1994. Kinematic analysis of a large-scale leading edge fold, Lost River Range, Idaho. Journal of Structural Geology 16, 337–354.

Geiser, P., Engelder, T., 1982. Distribution of layer-parallel shortening fabrics in Appalachian Foreland of New York and Pennsylvania: evidence for two noncoaxial phases of Alleghany Orogeny. AAPG Bulletin 66, 1168.

Ghosh, S.K., 1993. Structural Geology: Fundamentals and Modern Developments. Pergamon Press, Oxford.

Giles, K.A., Lawton, T.F., 2002. Halokinetic sequence stratigraphy adjacent to the El Papalote diapir, northeastern Mexico. America Association of Petroleum Geologists Bulletin 86, 823–840.

Goldhammer, R.K., Lehmann, P.J., Todd, R.G., Wilson, J.L., Ward, W.C., Johnson, C.R., 1991. Sequence Stratigraphy and Cyclostratigraphy of the Mesozoic of the Sierra Madre Oriental, Northeast Mexico, a Field Guidebook. Gulf Coast Section, Society of Economic Paleontologists and Mineralogists.

Gray, G.G., Johnson, C.A., 1995. Structural and Tectonic Evolution of the Sierra Madre Oriental, with Emphasis on the Saltillo-Monterrey Corridor, a Field Guidebook. American Association of Petroleum Geologists, Houston, TX.

Gray, G.G., Pottorf, R.J., Yurewicz, D.A., Mahon, K.I., Pevear, D.R., Chuchla, R.J., 2001. Thermal and chronological record of Syn- to Post-Laramide burial and exhumation, Sierra Madre Oriental, Mexico. In: Bartolini, C., Buffler, R.T., Cantú-Chapa, A. (Eds.), The Western Gulf of Mexico Basin: Tectonics, Sedimentary Basins, Petroleum Systems. AAPG Memoir 75, pp. 159–181.

Gray, M.G., Mitra, G., 1999. Ramifications of four-dimensional progressive deformation in contractional mountain belts. Journal of Structural Geology 21, 1151–1160.

Hardy, S., Poblet, J., 1994. Geometric and numerical model of progressive limb rotation in detachment folds. Geology 23, 371–374.

Higuera-Diaz, C., Fischer, M.P., Wilkerson, M.S., 2005. Geometry and kinematics of the Nuncios detachment fold complex: implications for lithotectonics in northeastern Mexico. Tectonics 24, TC4010, doi:10.1029/2003TC0011615.

Holl, J.E., Anastasio, D.J., 1995. Cleavage development within a foreland fold and thrust belt, southern Pyrenees, Spain. Journal of Structural Geology 17, 357–369.

Homza, X.T., Wallace, W.K., 1995. Geometric and kinematic models for detachment folds within fixed and variable detachment depths. Journal of Structural Geology 17, 575–588.

Homza, X.T., Wallace, W.K., 1997. Detachment folds within fixed and variable detachment depths, northeastern Brooks Range, Alaska. Journal of Structural Geology 19, 337–354.

Jamison, W.R., 1987. Geometric analysis of fold development in overthrust terranes. Journal of Structural Geology 9, 207–219.

Johnson, A.M., 1980. Folding and faulting of strain-hardening sedimentary rocks. Tectonophysics 62, 251–278.

Kligfield, R., Owens, W.H., Lowrie, W., 1981. Magnetic susceptibility anisotropy, strain and progressive deformation in Permian sediments from the Maritime Alps (France). Earth and Planetary Science Letters 55, 181–189.

Latta, D.K., 2005. Structural, lithotectonic, rock magnetic studies of décollement folding, Coahuila Marginal Folded Province, northeast Mexico. PhD dissertation, Lehigh University, Bethlehem, PA.

Longoria, J.F., 1998. The mesozoic of the Mexican Cordillera in Nuevo Leon, NE Mexico. In: Longoria, J.F., Krutak, P.R., Gamper, M.A. (Eds.), Geologic Studies in Nuevo Leon, Mexico. Sociedad Mexicana de Paleontologia. AC Special Publication, pp. 1–44.

Marrett, R.A., Aranda-García, M., 1999. Structure and kinematic development of the Sierra Madre Oriental fold-thrust belt. In: Wilson, J.L., Ward, W.C., Marrett, R.A. (Eds.), Stratigraphy and Structure of the Jurassic and Cretaceous Platform and Basin Systems of the Sierra Madre Oriental; Monterrey and Saltillo Areas, Northeastern Mexico; a Field Book and Related Papers. South Texas Geological Society, San Antonio, TX, pp. 69–98.

McBride, E.F., Weide, A.E., Wollenben, J.A., Laudon, R.C., 1974. Stratigraphy and structure of the Parras and La Popa Basin, northeast Mexico. Geological Society of America Bulletin 85, 1603–1622.

Mitra, S., 1987. Regional variations in deformation mechanisms and structural styles in the central Appalachian orogenic belt. Geological Society of America Bulletin 98, 569–590.

Mitra, S., Namson, J.S., 1989. Equal-area balancing. American Journal of Science 289, 563–599.

Mountjoy, E.W., 1960. Structure and stratigraphy of the Miette and adjacent areas, Jasper National Park, Alberta. PhD thesis, University of Toronto.

Nicklesen, R.P., 1963. Fold patterns and continuous deformation mechanisms of the central Pennsylvania folded Applachians. In: Wager, W.R., and Nicklesen, R.P. (Eds.), Tectonics and Cambrian-Ordovician stratigraphy Central Applachians of Pennsylvania: Guidebook; 1963 Field Conference Pittsburgh Geoloical Society, pp. 13-30.

Nickelsen, R.P., 1979. Sequence of structural stages of the Alleghany Orogeny, at the Bear Valley strip mine, Shamokin, Pennsylvania. American Journal of Science 279, 225–271.

Parés, J.M., van der Pluijm, B.A., 2002. Evaluating magnetic lineations (AMS) in deformed rocks. Tectonophysics 350, 283–298.

Pettijohn, F.J., 1975. In: Sedimentary Rocks, third ed. Harper and Row, New York, 628 pp.

Pindell, J.L., 1985. Alleghenian reconstructions and subsequent evolution of the Gulf of Mexico, Bahamas, proto-Caribbean. Tectonics 4, 1–39.

Ramberg, H., 1963. Strain distribution and geometry of folds. Geological Institute University of Uppsala Bulletin 42. 1–20.

Ramsay, J.G., 1967. Folding and Fracturing of Rocks. McGraw-Hill, New York.

Ramsay, J.G., Huber, M.I., 1987. Techniques of Modern Structural Geology – Strain Analysis. Academic Press, London.

Salvador, A., 1987. Late Triassic-Jurassic paleogeography and origin of the Gulf of Mexico Basin. American Association of Petroleum Geologists Bulletin 71, 419–451.

Salvini, F., Storti, F., 2004. Active-hinge-folding-related deformation and its role in hydrocarbon exploration and development; insights from HCA modeling. In: McClay, K.R. (Ed.), Thrust Tectonics and Hydrocarbon Systems. AAPG Memoir 82, pp. 453–472.

Schwerdtner, W.M., 1990. Structural test of diapir hypothesis in Archean crust of Ontarion. Canadian Journal of Earth Science 27, 387–402.

Suppe, J., Namson, J., 1979. Fault-bend origin of frontal folds of the western Taiwan fold-and-thrust belt. Petroleum Geology of Taiwan 16, 1–18.

Tavarnelli, E., 1999. Normal faults in thrust sheets: pre-orogenic extension, post-orogenic extension, or both? Journal of Structural Geology 21, 1011–1018.

Wall, J.R., Murray, G.E., Diaz, T., 1961. Geology of the Monterrey area, Nuevo Leon, Mexico. Transactions – Gulf Coast. Association of Geological Societies 11, 57–71.

Williams, P.F., 1977. Foliation: a review and discussion. Tectonophysics 39, 305–328.

Willis, B., 1892. The mechanics of Appalachian structure. United States Geological Survey 13th Annual Report, 1891–1892, pp. 213–281.

Wilson, J.L., 1990. Basement structural controls on Mesozoic carbonate facies in northeastern Mexico – a review. Special Publication of the International Association of Sedimentologists 9, 235–255.

Wilson, J.L., 1999. Controls on the wandering path of the Cupido Reef trend in northeastern Mexico. In: Bartolini, C., Wilson, J.L., Lawton, T.F. (Eds.), Mesozoic Sedimentary and Tectonic History of North-Central Mexico. Geological Society of America Special Paper 340, Boulder, CO, pp. 135–143.

Wilson, J.L., Ward, W.C., Finneran, J.M. (Eds.), 1984. A Field Guide to Upper Jurassic and Lower Cretaceous Carbonate Platform and Basin Systems, Monterrey-Saltillo Area, Northeast Mexico. Gulf Coast Section, Society of Economic Paleontologists and Mineralogists.

Wiltschko, D.V., 1979. A mechanical model for thrust sheet deformation at a ramp. Journal of Geophysical Research 84, 1091–1104.

Wiltschko, D.V., Chapple, W.M., 1977. Flow of weak rocks in the Appalachian Plateau folds. American Association of Petroleum Geologists Bulletin 61, 653–670.

Wood Jr., G.H., Bergin, M.J., 1970. Structural control of the Anthracite Region, Pennsylvania. In: Fisher, G.W., Pettijohn, F.J., Reed, J.C., Weaver, K.N. (Eds.), Studies of Appalachian Geology, Central and Southern. Wiley, New York.

Woodward, N.B., 1997. Low-amplitude evolution of break-thrust folding. Journal of Structural Geology 19, 293–301.

Woodward, N.B., Rutherford, E., 1989. Structural lithic units in external orogenic zones. Tectonophysics 158, 247–267.